Spectroscopic Properties of Photosynthetic Reaction Centers. 1. Theory

Arieh Warshel*† and William W. Parson*‡

Contribution from the Department of Chemistry, University of Southern California, Los Angeles, California 90007, and the Department of Biochemistry, University of Washington, Seattle, Washington 98195. *Received November 20, 1986*

Abstract: A theoretical basis is developed for evaluating the electronic states of the interacting pigments in the reaction centers of photosynthetic bacteria. The approach starts with the basis set of individual molecules and then constructs combined electronic states for the oligomeric system at the self-consistent-field/configuration-interaction (SCF/CI) level by considering intermolecular interactions including charge-transfer interactions. Molecular orbitals for the individual pigments (four molecules of bacteriochlorophyll-*b* and two molecules of bacteriopheophytin-*b* in the case of the reaction center of *Rhodopseudomonas viridis*) are obtained as linear combinations of atomic p_z orbitals, using the quantum-mechanical-consistent-force-field (QCFF/PI) method. Electric and magnetic transition dipoles for the optical transitions of the isolated molecules are calculated by using a gradient-operator treatment, and the configuration interaction (CI) coefficients for the two dominant configurations are adjusted so that the calculated dipole strengths of the Q_y and Q_x absorption bands agree with experimental values. This procedure provides a self-consistent and unbiased basis set for calculations of the oligomeric system. To construct π-electron wave functions for the reaction center, we describe the excited electronic states of the complex in terms of the local excitations of the individual molecules and intermolecular charge-transfer (CT) transitions. Interactions among the molecules are introduced in the form of a configuration interaction matrix **U**, whose off-diagonal elements describe the mixing of the local and CT transitions. General expressions for the matrix elements are developed in terms of the atomic p_z orbital coefficients, the CI coefficients for the individual molecules, and semiempirical Coulomb and resonance integrals. The elements describing exciton-type interactions between locally excited states of different molecules take the form of transition-monopole expressions, which are scaled to be consistent with the dipole strengths of the individual molecules. The dependence of the matrix elements on intermolecular distance is examined. At the short distance between two of the bacteriochlorophyll molecules in the *Rps. viridis* reaction center, the point-monopole treatment gives very different results than a point-dipole approximation for some of the matrix elements. Also, some of the matrix elements for the mixing of CT transitions with local transitions are found to be considerably larger than the exciton-type elements. The final expressions for the dipole strengths and rotational strengths for the complex take into account the intrinsic magnetic transition dipoles of the individual molecules and also include the contributions that doubly excited states make to the ground state of the complex. In the following paper [Parson and Warshel, accompanying paper], the theory is used to calculate the spectroscopic properties of *Rps. viridis* reaction centers.

The reaction centers of photosynthetic bacteria are pigment–protein complexes that carry out the initial electron-transfer steps of photosynthesis. Reaction centers have been purified from numerous species of bacteria (see ref 1–3 for reviews), and the crystal structure of reaction centers from *Rhodopseudomonas viridis* has recently been solved to 3.0-Å resolution.[4,5]

Reaction centers from many species contain three polypeptides (referred to as "L, M and H"), four molecules of bacteriochlorophyll (BChl), two molecules of bacteriopheophytin (BPh), two quinones, and one non-heme iron atom.[1-3] In some bacterial species, such as *Rps. viridis*, the pigments are bacteriochlorophyll *b* and bacteriopheophytin *b* (BChl-*b* and BPh-*b*); more commonly, they are bacteriochlorophyll *a* and bacteriopheophytin *a*. In all cases, however, two of the four BChls appear to form a "special pair" (P) that interact particularly strongly with each other. In the *Rps. viridis* crystal structure,[4,5] the two molecules that make up P ($BChl_{LP}$ and $BChl_{MP}$) are centered about 7.1 Å apart Figure 1). Their molecular planes are approximately parallel. An axis of local C_2 pseudosymmetry passes between $BChl_{LP}$ and $BChl_{MP}$ and extends to the Fe atom, about 20 Å away. The other two BChls ($BChl_{LA}$ and $BChl_{MA}$), the two BPhs (BPh_L and BPh_M), and the quinones sit in the region between P and the Fe, with $BChl_{LA}$ and BPh_L on the side of the symmetry axis that is formed mainly by the L polypeptide and $BChl_{MA}$ and BPh_M on the side formed mainly by M. When the reaction center is excited with light, P transfers an electron to BPh_L with a time constant of 3 to 4 ps.[6-8] An electron subsequently hops from BPh_L to one of the quinones, and from there to the second quinone.

The spectroscopic properties of reaction centers differ significantly from those of the monomeric pigments in solution. The long-wavelength (Q_y) absorption band of monomeric BChl-*b* in ether occurs at approximately 780 nm, has a dipole strength of about 50 D^2, and has negligible rotational strength. The long-wavelength band of *Rps. viridis* reaction centers occurs near 960 nm at room temperature and has a dipole strength of about 100 D^2 and a rotational strength of about 4 $D\cdot\mu_B$. Because of this band bleaches when P is oxidized to P^+, it is generally attributed to the two BChls of the special pair. Whether the large red shift of the band is due predominantly to exciton interactions between the BChls, to charge-transfer interactions, or to interactions of the pigments with the protein has been the subject of considerable experimental work and theoretical consideration,[2,9-26] but it has

† University of Southern California.
‡ University of Washington.

(1) Feher, G.; Okamura, M. Y. In *The Photosynthetic Bacteria*; Clayton, R. K., Sistrom, W. R., Eds.; Plenum: New York, 1978; pp 349–386.
(2) Parson, W. W. *Annu. Rev. Biophys. Bioeng.* **1982**, *11*, 57–80.
(3) Parson, W. W. In *Photosynthesis*; Amesz, J., Ed.; Elsevier: Amsterdam, 1987; pp 43–61.
(4) Deisenhofer, J.; Epp, O.; Miki, K.; Huber, R.; Michel, H. *J. Mol. Biol.* **1984**, *180*, 385–398.
(5) Michel, H.; Epp, O.; Deisenhofer, J. *EMBO J.* **1986**, *5*, 2445–2451.
(6) Woodbury, N. W.; Becker, M.; Middendorf, D.; Parson, W. W. *Biochemistry* **1985**, *24*, 7516–7521.
(7) Martin, J.-L.; Breton, J.; Hoff, A.; Migus, A.; Antonetti, A. *Proc. Natl. Acad. Sci. U.S.A.* **1986**, *83*, 957–961.
(8) Breton, J.; Martin, J.-L.; Migus, A.; Antonetti, A.; Orszag, A. *Proc. Natl. Acad. Sci. U.S.A.* **1986**, *83*, 5121–5125.
(9) Vermeglio, A.; Clayton, R. K. *Biochim. Biophys. Acta* **1976**, *449*, 500–515.
(10) Vermeglio, A.; Breton, J.; Paillotin, G.; Cogdell, R. J. *Biochim. Biophys. Acta* **1978**, *501*, 514–530.
(11) Shuvalov, V. A.; Asadov, A. A. *Biochim. Biophys. Acta* **1979**, *545*, 296–308.
(12) Warshel, A. *J. Am. Chem. Soc.* **1979**, *101*, 744–746.
(13) Warshel, A. *Proc. Natl. Acad. Sci. U.S.A.* **1980**, *77*, 3105–3109.
(14) Thornber, J. P.; Cogdell, R. J.; Seftor, R. E. B.; Webster, G. D. *Biochim. Biophys. Acta* **1980**, *593*, 60–75.
(15) Pearlstein, R. In *Photosynthesis, Energy Conversion by Plants and Bacteria*; Govindjee, Ed.; Academic: New York, 1982; pp 293–330.
(16) Breton, J.; Vermeglio, A. In *Photosynthesis, Energy Conversion by Plants and Bacteria*; Govindjee, Ed.; Academic: New York, 1982; pp 153–194.

0002-7863/87/1509-6143$01.50/0

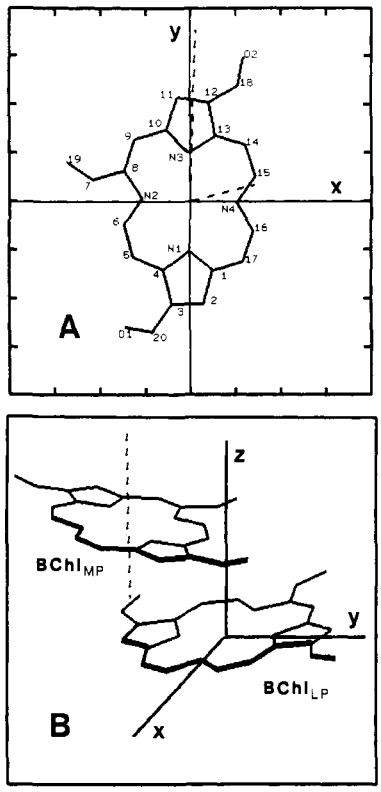

Figure 1. (A) Numbering scheme used for the 26 atoms of the π system of BChl-*b*. The diagram shows a planar projection of the conjugated portion of the molecule, based on the atomic coordinates of BChl$_{LP}$ of the *Rps. viridis* reaction center.[4,5] The normal to the plane is defined by the cross product of the N2 → N4 and N1 → N3 vectors; the latter vector provides the *y*-axis of the figure. The scale markers on the frame of the figure are in intervals of 2 Å. The dashed lines show the Q_y and Q_x transition dipole vectors calculated with eq 8 of the text; for these, the scale markers represent intervals of 2 D. (B) Geometry of the special pair of BChls (BChl$_{LP}$ and (BChl$_{MP}$) in the *Rps. viridis* reaction center. The Cartesian coordinate system is defined with reference to BChl$_{LP}$ as in part A. The dashed line passing through the center of BChl$_{MP}$ is parallel to the cross product of the N1 → N3 vectors of the two BChls.

remained unresolved. *Rps. viridis* reaction centers also have 5 or more overlapping absorption bands in the region between 790 and 860 nm, and it has been unclear whether some of these bands can be assigned individually to BChl$_{LA}$, BChl$_{MA}$, BPh$_L$, and BPh$_M$ or whether they are exciton bands that include contributions from BChl$_{LP}$ and BChl$_{MP}$.

In order to obtain a fundamental understanding of the electronic states of bacterial reaction centers, it is necessary to go beyond the point-dipole approximations that have been used in most of the previous theoretical studies of such systems.[2,15,18-23] It also is of interest to explore how intermolecular charge-transfer (CT) transitions contribute to the reaction center's spectroscopic properties, because of the potential importance of these interactions in the photochemical electron-transfer reaction. A realistic analysis of these topics requires a quantum mechanical evaluation of the energy levels of six interacting BChl and BPh molecules, which is not a simple task. Although ab initio calculations of the ground states of chlorophyll monomers are feasible,[27,28] reliable calculations of the excited states of a monomer require a very large basis set and extensive configuration interactions and are extremely demanding of computer time. Ab initio calculations of the excited states of a BChl dimer do not seem feasible at present unless they are performed with a severely restricted basis set. The use of a limited basis set leads to substantial overestimates of the excitation energies, necessitating an "empirical" scaling of the results.[28] The ground state of a chlorophyll dimer was studied recently by a semiempirical all-valence-electrons method,[29] but this study still required extensive computer time and did not evaluate the excited electronic surfaces of the dimer.

At present, the most practical and probably the most reliable way of studying systems the size of a BChl dimer appears to be the quantum-mechanical-consistent-force-field/π-electron (QCFF/PI) method.[30-33] This method has been used to evaluate the potential surfaces and Franck–Condon factors of chlorophyll dimers, as well as the solvation of such a dimer by a microscopic nonpolar environment.[12,13] However, the QCFF/PI "supermolecule" treatment does not provide a practical strategy for studying the electronic states for complexes larger than a dimer. Thus, in order to explore the spectroscopic properties of the bacterial reaction center we have sought a new theoretical approach. The theory presented below, which is still on the level of a self-consistent-field/configuration-interaction (SCF/CI) treatment, provides a convenient connection between the properties of the isolated monomeric molecules and the properties of the interacting system. This is achieved by first obtaining the molecular orbitals of the individual BChl and BPh molecules with use of the QCFF/PI method and then constructing the intermolecular interaction matrix, considering CT transitions explicitly in addition to the interactions between the excited states of the individual pigments. This treatment differs from previous theoretical work on reaction centers both in including CT states and in using a point-monopole expression for intermolecular interactions in place of a point-dipole approximation.

Our approach represents an attempt to address some of the key questions about the reaction center without simply adjusting a set of parameters to reproduce the relevant observables. Since perfect wave functions cannot be obtained at present by any model, we scale the wave functions of the individual monomers to fit *their* observed spectroscopic properties and then use these wave functions to calculate the properties of the oligomeric system. Such an approach avoids introducing any bias toward the properties of the oligomer. The theory is described in general terms in the present paper, and it is applied to *Rps. viridis* reaction centers in the following paper.[34] A preliminary report has outlined the theory and described some of our conclusions.[22]

Theoretical Method

Monomer Wave Functions and Transition Dipoles. Wave functions for isolated BChl and BPh monomers were obtained by the QCFF/PI method,[30-33] using the simplified heteroatom parameters given in Table IV of ref 33. This method evaluates the π-electron wave function by a Pariser–Parr–Pople-type approach

(17) Eccles, J.; Honig, B. *Proc. Natl. Acad. Sci. U.S.A.* **1983**, *80*, 4959-4962.
(18) Mar, T.; Gingras, G. *Biochim. Biophys. Acta* **1984**, *764*, 283-294.
(19) Scherz, A.; Parson, W. W. *Biochim. Biophys. Acta* **1985**, *766*, 666-678.
(20) Knapp, E. W.; Fischer, S. F. In *Antennas and Reaction Centers of Photosynthetic Bacteria*; Michel-Beyerle, M. E., Ed.; Springer-Verlag: Berlin, 1985; pp 103-108.
(21) Knapp, E. W.; Fischer, S. F.; Zinth, W.; Sander, M.; Kaiser, W.; Deisenhofer, J.; Michel, H. *Proc. Natl. Acad. Sci. U.S.A.* **1985**, *82*, 8463-8467.
(22) Parson, W. W.; Scherz, A.; Warshel, A. In *Antennas and Reaction Centers of Photosynthetic Bacteria*; Michel-Beyerle, M. E., Ed.; Springer-Verlag: Berlin, 1985; pp 122-130.
(23) Breton, J. *Biochim. Biophys. Acta* **1985**, *801*, 235-245.
(24) Hoff, A.; Lous, E. J.; Moehl, K. W.; Dijkman, J. A. *Chem. Phys. Lett.* **1985**, *114*, 39-43.
(25) Kirmaier, C.; Holten, D.; Parson, W. W. *Biochim. Biophys. Acta* **1985**, *810*, 49-61.
(26) Knapp, E. W.; Scherer, P. O. J.; Fischer, S. F. *Biochim. Biophys. Acta* **1986**, *852*, 295-305.
(27) Kashiwagi, H.; Hirota, F.; Nagashima, U.; Takada, T. *Int. J. Quantum Chem.* **1986**, *30*, 311-326.
(28) Petke, J. D.; Maggiora, G. M. *J. Chem. Phys.* **1986**, *84*, 1640-1652.
(29) Plato, M.; Trankle, E.; Lubitz, W.; Lendzian, F.; Mobius, K. *Chem. Phys.* **1986**, *107*, 185-196.
(30) Warshel, A.; Karplus, M. *J. Am. Chem. Soc.* **1972**, *94*, 5612-5625.
(31) Warshel, A. *Comp. Chem.* **1977**, *1*, 195-202.
(32) Warshel, A. In *Modern Theoretical Chemistry*; Segal, G., Ed.; Plenum: New York, 1977; Vol. 7, Part A, pp 133-172.
(33) Warshel, A.; Lappicirella, V. A. *J. Am. Chem. Soc.* **1981**, *103*, 4664-4673.
(34) Parson, W. W.; Warshel, A. *J. Am. Chem. Soc.*, following paper in this issue.

corrected for overlap between bonded atoms and modified to include the effect of the residual charges of the π-electrons and the charge of the central Mg or H atoms. The method has been used extensively in studies of porphyrins and other conjugated molecules, and it has given reliable results for structures, energetics, vibrations, and other properties.[32,33] Molecular orbitals of the individual molecules are written as linear combinations of atomic orbitals

$$\phi_n = \sum_t v_{n,t}\chi_t \tag{1}$$

where χ_t is a p_z orbital on atom t. The expansion coefficients $v_{n,t}$ are obtained by solving the self-consistent-field (SCF) equation, which in matrix form is

$$\mathbf{F}\mathbf{v}_n = E_n\mathbf{v}_n \tag{2a}$$

where $\mathbf{F}$ is the Fock Hamiltonian (eq. 4 of [30]) and E_n is the energy of molecular orbital n. The elements of $\mathbf{F}$ are given by

$$\mathbf{F}_{t,t} = \alpha_{t,t} + (1/2)\gamma_{t,t}P_{t,t} - \sum_{s\neq t}\gamma_{t,s}q_s \tag{2b}$$

$$\mathbf{F}_{t,s} = \beta_{t,s} - (1/2)\gamma_{t,s}P_{t,s} \tag{2c}$$

Here $\alpha_{t,t}$ is the effective ionization energy ($\alpha_{t,t} \equiv \mathbf{H}_{t,t\,\mathrm{core}}$); $P_{t,s}$ is the bond order ($P_{t,s} = 2\sum_n^{\mathrm{occ}} v_{n,t}v_{n,s}$, with the sum running over the occupied orbitals); the q_s are the atomic charges; $\beta_{t,s}$ is the resonance integral between the p_z orbitals on atoms t and s ($\beta_{t,s} = \mathbf{H}_{t,s\,\mathrm{core}} = \int \chi_t(1)\mathrm{H}_{\mathrm{core}}\chi_s(1)\,\mathrm{d}\tau_1$); and $\gamma_{t,s}$ is the electron–electron repulsion integral ($\gamma_{t,s} = \int\int \chi_s(1)\chi_s(1)(1/r_{12})\chi_t(2)\chi_t(2)\,\mathrm{d}\tau_1\,\mathrm{d}\tau_2$). The semiempirical expressions used for β and γ are discussed below; see ref 30 for additional details.

The major optical absorption bands of BChl and BPh are due largely to transitions involving the top two filled molecular orbitals and the two lowest unfilled orbitals.[35-38] We shall refer to these four orbitals as ϕ_1 to ϕ_4 in order of increasing energy. The expansion coefficients $v_{n,t}$ for ϕ_1 to ϕ_4 of BChl-*b* and BPh-*b* are listed in Table I. Figure 1A shows the scheme used for numbering the conjugated atoms.

Wave functions for the excited states of an individual BChl or BPh molecule can be written as

$$\Psi_i = \sum_N c_{i,N}{}^1\psi_N \tag{3}$$

where ${}^1\psi_N \equiv {}^1\psi_{n1\to n2}$ represents the singlet wave function corresponding to excitation from SCF orbital n_1 to n_2. The configuration-interaction (CI) coefficients $c_{i,N}$ are obtained (see, e.g., ref 32 and 39) by solving the equation

$$\mathbf{A}\mathbf{c}_i = \Delta E_i\mathbf{c}_i \tag{4}$$

where the ΔE_i are the excitation energy eigenvalues and the matrix elements of $\mathbf{A}$ are given by

$$\begin{aligned}\mathbf{A}_{N,N} &= \langle {}^1\psi_{n1\to n2}|\mathrm{H}|{}^1\psi_{n1\to n2}\rangle - \langle\psi_0|\mathrm{H}|\psi_0\rangle \\ &= E_{n2} - E_{n1} + 2\langle \mathrm{n_1n_2}|\mathrm{n_2n_1}\rangle - \langle \mathrm{n_1n_2}|\mathrm{n_1n_2}\rangle\end{aligned} \tag{5a}$$

$$\mathbf{A}_{N,M} = \langle {}^1\psi_{n1\to n2}|\mathrm{H}|{}^1\psi_{m1\to m2}\rangle = 2\langle \mathrm{m_1n_2}|\mathrm{m_2n_1}\rangle - \langle \mathrm{m_1n_2}|\mathrm{n_1m_2}\rangle \tag{5b}$$

Here ψ_0 is the wave function for the zero-order ground state, and

$$\begin{aligned}\langle mn|pq\rangle &= \int\int \phi_{\mathrm{m}}(1)\phi_{\mathrm{n}}(2)(1/r_{12})\phi_{\mathrm{p}}(1)\phi_{\mathrm{q}}(2)\,\mathrm{d}\tau_1\,\mathrm{d}\tau_2 \\ &\approx \sum_{s,t} v_{m,s}v_{n,t}v_{p,s}v_{q,t}\gamma_{s,t}\end{aligned} \tag{6}$$

For BChl or BPh, the solution of eq 4 (diagonalization of $\mathbf{A}$) gives four main excited states called Q_y, Q_x, B_x, and B_y. The Q_y and B_y transitions are due mainly to excitations from ϕ_2 to ϕ_3 and from ϕ_1 to ϕ_4; the Q_x and B_x transitions are due mainly to excitations from ϕ_2 to ϕ_4 and from ϕ_1 to ϕ_3. With the molecular orbitals of Table I, the calculated excitation energies for BChl-*b* are 15 290 cm^{-1} for Q_y, 16 790 for Q_x, 29 870 for B_x, and 32 250 for B_y. The experimentally measured 0–0 transition energies are approximately 12 200, 16 700, 24 000, and 26 600 cm^{-1} for BChl-*b* in ether.[22] The calculations thus estimate the energy of the Q_x transition well, but they tend to overestimate the energies of the other transitions. For BPh-*b*, the calculated energies are 14 170, 16 990, 29 910, and 37 520 cm^{-1}; experimental values are 12 400, 16 800, 24 000, and 26 600 cm^{-1} [A. Scherz, personal communication].

Table I. Molecular Orbital Coefficients for BChl-*b* and BPh-*b*

atom	ϕ_1	ϕ_2	ϕ_3	ϕ_4
		BChl-*b*		
1	0.0721	−0.2967	0.2065	−0.1081
2	−0.0794	−0.2185	0.2830	−0.0039
3	−0.1000	0.2070	−0.2407	0.0916
4	0.0409	0.3044	−0.1700	−0.1885
5	0.3651	−0.0560	0.2754	−0.2064
6	0.1153	−0.3076	0.1298	0.2903
7	−0.0016	−0.0122	0.0460	−0.2507
8	0.0540	0.3224	0.1607	−0.3195
9	0.3465	0.1130	0.2407	0.3624
10	0.0872	−0.3041	−0.2076	0.1171
11	−0.0675	−0.2213	−0.2709	−0.2172
12	−0.1075	0.1882	0.2177	0.0287
13	0.0238	0.2950	0.1760	0.1910
14	0.3804	−0.0321	−0.2374	0.1290
15	0.1084	−0.2811	−0.1159	−0.2641
16	0.0778	0.2954	−0.1480	0.2019
17	0.3803	0.0996	−0.2421	−0.1663
18	−0.0191	0.0416	0.1308	0.0466
19	−0.0363	−0.2114	−0.1120	0.3554
20	−0.0161	0.0492	−0.1493	0.1492
N1	−0.2548	−0.0107	−0.0414	0.2120
N2	−0.3275	−0.0094	−0.2996	0.0161
N3	−0.2498	−0.0291	0.0160	−0.2313
N4	−0.3648	−0.0294	0.2761	0.0414
O1	0.0538	−0.1095	0.1619	−0.1246
O2	0.0575	−0.1009	−0.1434	−0.0389
		BPh-*b*		
1	0.0021	−0.3410	0.2756	−0.1149
2	−0.0569	−0.2020	0.2305	0.0212
3	−0.0565	0.2087	−0.2228	0.0885
4	−0.0127	0.3542	−0.2632	−0.1248
5	0.3141	−0.0023	0.1830	−0.2305
6	0.2170	−0.3199	0.2413	0.2349
7	−0.0673	−0.0376	0.0221	−0.2004
8	0.1500	0.3171	0.2704	−0.3334
9	0.3607	0.0520	0.1805	0.3831
10	0.0720	−0.3160	−0.2900	0.1008
11	−0.0390	−0.1804	−0.2424	−0.1926
12	−0.0989	0.1705	0.2087	0.0068
13	−0.0627	0.2998	0.2704	0.2260
14	0.3577	0.0075	−0.1387	0.1999
15	0.2442	−0.2480	−0.2108	−0.3153
16	0.2157	0.2912	−0.2232	0.2005
17	0.3539	0.0413	−0.1400	−0.1902
18	0.0024	0.0187	0.0693	0.0052
19	−0.1333	−0.2128	−0.1792	0.3427
20	0.0041	0.0266	−0.0750	0.0714
N1	−0.2737	−0.0170	−0.0290	0.1975
N2	−0.2281	0.0015	−0.2301	0.0340
N3	−0.2825	−0.0307	−0.0151	−0.2693
N4	−0.2859	−0.0210	0.1948	0.0409
O1	0.0344	−0.1079	0.1197	−0.0737
O2	0.0577	−0.0887	−0.1127	−0.0064

The electric transition dipole for the excitation to ψ_i is frequently calculated as

$$\begin{aligned}\mu_i &= \langle\psi_i|e\mathbf{r}|\psi_0\rangle \\ &\approx \sqrt{2}\sum_{N,t} c_{i,N}\langle\psi_{n2}|e\mathbf{r}|\psi_{n1}\rangle \approx e\sqrt{2}\sum_{N,t} c_{i,N}v_{n1,t}v_{n2,t}\mathbf{r}_t\end{aligned} \tag{7}$$

where $\mathbf{r}$ is the electron position and $\mathbf{r}_t$ is the position of atom t. However, it has been pointed out[41,42] that dipole strengths (D_i =

(35) Gouterman, M. *J. Mol. Spectrosc.* **1961**, *6*, 138–163.
(36) Weiss, C.; Kobayashi, H.; Gouterman, M. *J. Mol. Spectrosc.* **1965**, *16*, 415–450.
(37) Weiss, C. *J. Mol. Spectrosc.* **1972**, *44*, 37–80.
(38) Petke, J. D.; Maggiora, G. M.; Shipman, L. L.; Christofferson, R. E. *Photochem. Photobiol.* **1980**, *32*, 399–414.
(39) Mataga, N.; Kubota, T. *Molecular Interactions and Electronic Spectra*; Marcel Dekker: New York, 1970; pp 64–65.
(40) Murrell, J. N.; Tanaka, J. *Mol. Phys.* **1964**, *7*, 363–380.
(41) McHugh, A. J.; Gouterman, M. *Theor. Chim. Acta* **1969**, *13*, 249–258.

Table II. Simplified CI Coefficients for BChl-*b* and BPh-*b*

	1 → 3	1 → 4	2 → 3	2 → 4
		BChl-*b*		
Q_y	0	-0.408	0.913	0
Q_x	0.907	0	0	0.422
B_x	-0.422	0	0	0.907
B_y	0	0.913	0.408	0
		BPh-*b*		
Q_y	0	-0.231	0.973	0
Q_x	0.871	0	0	0.492
B_x	-0.492	0	0	0.871
B_y	0	0.973	0.231	0

$|\mu_i|^2$) calculated with eq 7 generally overestimate experimentally measured dipole strengths, and we found this to be the case in the present work. Better agreement with the experimental values can be obtained by using the transition gradient operator.

$$\mu_i = [h^2/m(\Delta E_i)]\langle\psi_i|e\nabla|\psi_0\rangle \approx [eh^2/m(\Delta E_i)]\sqrt{2}\sum_N c_{i,N}[2\sum_\kappa(v_{n1,\kappa1}v_{n2,\kappa2} - v_{n2,\kappa1}v_{n1,\kappa2})(\mathbf{b}_\kappa/b_\kappa)|\cos\varphi_\kappa|\mathbf{I}(b_\kappa)] \quad (8)$$

Here the second sum runs over all of the conjugated bonds in the molecule; $\kappa1$ and $\kappa2$ are bonded atoms; $\mathbf{b}_\kappa$ is the vector (with length b_κ) from atom $\kappa1$ to atom $\kappa2$; φ_κ is the torsional angle of the atomic p_z axes through $\mathbf{b}_\kappa$. (The absolute value of cos φ_κ is taken in order to be consistent with the QCFF/PI calculations, where all of the p_z orbitals are considered to point above the molecular plane.) The function $\mathbf{I}(b_\kappa)$ is given by

$$\mathbf{I}(b_\kappa) = \int p_z^{\kappa1}(\partial p_z^{\kappa2}/\partial x)\,d\tau \approx \exp(-\rho)(1 + 0.850\rho + 0.494\rho^2 + 0.077\rho^3) \quad (9)$$

with $\rho = 3.07b_\kappa/$Å. Expressions similar to eq 8 and 9 have been used previously by McHugh and Gouterman,[41,42] Chong,[43] and Schlessinger and Warshel.[44]

Our goal is to explore intermolecular interactions in the reaction center by using the most reliable wave functions for the monomeric pigments. Since the calculated wave functions of the monomers are not exact, we can improve them by adjusting the CI coefficients ($c_{i,N}$) so as to optimize the agreement between the dipole strengths calculated with eq 8 and the monomers' experimentally measured dipole strengths. To simplify the model and the subsequent calculations on oligomers, we used only the two main configurations for each transition. Experimental dipole strengths for the Q_y and Q_x transitions of monomeric BChl-*b* in ether are approximately 50 and 8.5 D^2, respectively;[22] those of BPh-*b* are approximately 38 and 7.6 D^2 [A. Scherz, personal communication]. These values can be matched by using eq 8 (with the experimental transition energies) and the CI coefficients listed in Table II. Using the same CI coefficients with eq 7 gives dipole strengths that are typically between 2- and 3-times larger than the values obtained with eq 8. (For comparison with the values in Table II, the unadjusted CI coefficients obtained from eq 4 along with the calculated transition energies were -0.381 and 0.924 for the Q_y transition of BChl-*b* and 0.878 and 0.477 for Q_x. Using these coefficients with the experimental energies and eq 8 gives dipole strengths of 58 and 4 D^2, respectively.)

Although this adjustment of the CI coefficients may appear "empirical", it does not represent a parametrization of the spectroscopic properties of the oligomer, but rather a consistent search for the best wave functions for the monomers. This procedure is particularly important if one wishes to explore charge-transfer interactions, since calculations of these interactions are sensitive to errors in the wave functions.

Because the B_x and B_y transitions are not well resolved in the absorption spectra, their dipole strengths are uncertain.[19] We therefore did not attempt to refine the $c_{i,N}$ for these transitions independently but rather used the values obtained by a simple symmetry transformation on the Q_y and Q_x coefficients (see Table II). The unrefined coefficients obtained directly by diagonalizing **A** obey this transformation closely. The coefficients listed in Table II give dipole strengths of approximately 100 and 75 D^2 for the B_x and B_y transitions of BChl-*b* and 116 and 53 D^2 for those of BPh-*b*. The sums of the B_x and B_y dipole strengths are reasonably close to the integrated experimental dipole strengths in this region of the spectrum (approximately 120 D^2 for BChl-*b* and 170 for BPh-*b* [A. Scherz, personal communication]).

The orientations of the calculated Q_y and Q_x transition dipoles of BChl-*b* are indicated in Figure 1. This illustration uses the atomic coordinates of $BChl_{LP}$ of the *Rps. viridis* reaction center;[4,5] the calculated dipole strengths and orientations vary slightly among the four BChl molecules. For $BChl_{LP}$, the Q_y dipole is aligned about 2° off the N1–N3 vector; the Q_x dipole is about 16° from the N2–N4 vector and makes an angle of 74° with the Q_y dipole. The latter angle agrees with the angle of 74 ± 2° that has been measured for BChl-*a* by fluorescence polarization,[45] but no experimental data on this point are available for BChl-*b*.

The magnetic transition dipole for excitation of the isolated molecule to ψ_i is

$$\mathbf{m}_i = -(ehi/4\pi mc)\langle\psi_i|\mathbf{r}\times\nabla|\psi_0\rangle \approx -(ehi/4\pi mc)\sqrt{2}\sum_N c_{i,N}\{2\sum_\kappa(v_{n1,\kappa1}v_{n2,\kappa2} - v_{n2,\kappa1}v_{n1,\kappa2})\times[\mathbf{r}_\kappa\times(\mathbf{b}_\kappa/b_\kappa)|\cos\varphi_\kappa|\mathbf{I}(b_\kappa) - (\mathbf{b}_\kappa/b_\kappa)|\sin\varphi_\kappa|\mathbf{S}(b_\kappa)]\} \quad (10)$$

where $\mathbf{S}(b_\kappa)$ is the overlap integral between two parallel $2p_z$ orbitals.[44] Since BChl and BPh are nearly planar, sin φ_κ is close to zero for most of the bonds and contributions from the term in $\mathbf{S}(b_\kappa)$ are negligible. We included this term only when we explored the effects of rotating the acetyl group on ring I.[34] The overlap integral for atoms 3 and 20 then was taken to be 0.2.

The rotational strength of the transition to ψ_i is given by

$$\mathcal{R}_i = -\mathrm{Im}[\mu_i\cdot\mathbf{m}_i] \quad (11)$$

where Im means the imaginary part of the quantity in the brackets. By using the gradient operator in the expressions for both μ_i and $\mathbf{m}_i$ (eq 8 and 10), one ensures that $\mathcal{R}$ will be independent of the choice of the origin of the coordinate system. $\mathcal{R}$ is relatively small for the Q and B transitions of BChl and BPh, because μ is approximately in the plane of the macrocycle whereas $\mathbf{m}$ is approximately perpendicular to the plane. The calculated values of $\mathcal{R}$ for the Q_y transition of the four BChl-*b* molecules in the *Rps. viridis* reaction center were on the order of ±0.03 $D\cdot\mu_B$.

Dimer Wave Functions. In treating an oligomer, we have the option of considering all of the monomers together as a supermolecule and obtaining molecular orbitals for the entire complex. Although this approach can lead to useful results,[12,13,28,29,46-48] it is impractical for complexes larger than a dimer and for widely separated molecules. In addition, it produces the final mixed states directly, without providing a description of the interaction between intramolecular π–π^* transitions and intermolecular charge-transfer (CT) transitions. It is helpful to preserve a distinction between these two types of transitions, if one wishes to obtain a clear picture of how excitation of the reaction center leads to intermolecular electron transfer. We therefore have explored the alternative approach of starting with molecular orbitals for the monomers, without including interactions between the individual molecules.

For monomers *a* and *b* in a dimer we write the zero-order molecular orbitals as

$$\phi^a{}_n = \sum_t v_{n,t}\chi^a{}_t \text{ and } \phi^b{}_m = \sum_s v_{m,s}\chi^b{}_s \quad (12)$$

just as in eq 1 and 2 except that *t* and *s* now represent atoms on

(42) McHugh, A. J.; Gouterman, M.; Weiss, C. *Theor. Chim. Acta* **1972**, *24*, 346–370.
(43) Chong, D. P. *Mol. Phys.* **1968**, *14*, 275–280.
(44) Schlessinger, J.; Warshel, A. *Chem. Phys. Lett.* **1974**, *28*, 380–383.
(45) Breton, J.; Vermeglio, A.; Garrigos, M.; Paillotin, G. *Proc. Int. Photosynth. Congr., 5th* **1980**, *3*, 445–459.
(46) Salem, L. *J. Am. Chem. Soc.* **1968**, *90*, 543–552.
(47) Warshel, A.; Huler, A. *Chem. Phys.* **1974**, *6*, 463–468.
(48) Warshel, A.; Shakked, Z. *J. Am. Chem. Soc.* **1975**, *97*, 5679–5684.

the two different molecules. This can be expressed in vector notation as $\mathbf{v}^a{}_n = (\mathbf{v}^a{}_n, \mathbf{0})$, $\mathbf{v}^b{}_m = (\mathbf{0}, \mathbf{v}^b{}_m)$. In this representation, the SCF **F** matrix has the form

$$\mathbf{F} = \begin{array}{c} \begin{matrix} \chi^a{}_t \cdots & \chi^b{}_s \cdots \end{matrix} \\ \left[\begin{matrix} \mathbf{F}^{aa} & \mathbf{F}^{ab} \\ \mathbf{F}^{ba} & \mathbf{F}^{bb} \end{matrix}\right] \end{array} = \begin{array}{c} \begin{matrix} \chi^a{}_t \cdots & \chi^b{}_s \cdots \end{matrix} \\ \left[\begin{matrix} \mathbf{F}^{aa} & \mathbf{H}^{ab}{}_{\text{core}} \\ \mathbf{H}^{ab}{}_{\text{core}} & \mathbf{F}^{bb} \end{matrix}\right] \end{array} \quad (13a)$$

where the elements of the Huckel matrix, $\mathbf{H}^{ab}{}_{\text{core}}$, are

$$\mathbf{H}^{ab}{}_{t,s\ \text{core}} = \beta_{t,s} \quad (13b)$$

The simplification of $\mathbf{F}^{ab}$ to $\mathbf{H}^{ab}{}_{\text{core}}$ in eq 13a is obtained because the off-diagonal bond orders $\mathbf{p}^{ab}$ are zero in our selection of the restricted molecular orbitals (see eq 2). This nonstandard approach, which is an essential part of our treatment, means that the **F** matrix is *not* diagonalized by the molecular orbital vectors **v**.

The interaction between the monomers can be introduced at the level of configuration interaction by writing a CI matrix for the dimer, $\mathbf{A}^{\mathrm{D}}$, in the form

$$\mathbf{A}^{\mathrm{D}} = \begin{array}{c} \begin{matrix} {}^1\psi^{aa}{}_N \cdots & {}^1\psi^{bb}{}_M \cdots & {}^1\psi^{ab}{}_{N'} \cdots & {}^1\psi^{ba}{}_{M'} \cdots \end{matrix} \\ \left[\begin{matrix} \mathbf{A}^{aa,aa} & \mathbf{A}^{aa,bb} & \mathbf{A}^{aa,ab} & \mathbf{A}^{aa,ba} \\ \mathbf{A}^{bb,aa} & \mathbf{A}^{bb,bb} & \mathbf{A}^{bb,ab} & \mathbf{A}^{bb,ba} \\ \mathbf{A}^{ab,aa} & \mathbf{A}^{ab,bb} & \mathbf{A}^{ab,ab} & \mathbf{A}^{ab,ba} \\ \mathbf{A}^{ba,aa} & \mathbf{A}^{ba,bb} & \mathbf{A}^{ba,ab} & \mathbf{A}^{ba,ba} \end{matrix}\right] \end{array} \quad (14)$$

Here $\mathbf{A}^{aa,aa}$ and $\mathbf{A}^{bb,bb}$ are the CI matrices for the isolated monomers (just as in eq 4–6). Charge-transfer (CT) transitions in which an electron moves from molecular orbital $n1'$ of molecule a to orbital $n2'$ of molecule b are written as ${}^1\psi^{ab}{}_{N'}$, and their energies are included as diagonal terms in the submatrix $\mathbf{A}^{ab,ab}$. CT transitions from orbital $m1'$ of molecule b to orbital $m2'$ of molecule a (${}^1\psi^{ba}{}_{M'}$) are included similarly in $\mathbf{A}^{ba,ba}$. The off-diagonal terms of $\mathbf{A}^{\mathrm{D}}$ contain the interaction matrix elements, which are given for $N \neq M$ by[49]

$$\begin{aligned} \mathbf{A}^{\mathrm{D}}{}_{N,M} = \delta_{n1,m1}\mathbf{F}_{n2,m2} - \delta_{n2,m2}\mathbf{F}_{n1,m1} + 2\langle \mathrm{m_1n_2}|\mathrm{m_2n_1}\rangle - \\ \langle \mathrm{m_1n_2}|\mathrm{n_1m_2}\rangle = \delta_{n1,m1}\sigma_{n2,m2} - \\ \delta_{n2,m2}\sigma_{n1,m1} + 2\langle \mathrm{m_1n_2}|\mathrm{m_2n_1}\rangle - \langle \mathrm{m_1n_2}|\mathrm{n_1m_2}\rangle \end{aligned} \quad (15)$$

Here $\sigma_{n1,m1}$ and $\sigma_{n2,m2}$ are the contributions from the overlap between the monomers.

$$\begin{aligned} \sigma_{nj,mk} = \mathbf{F}_{nj,mk} &= \textstyle\sum_{t,s}\mathrm{v}_{nj,t}\mathrm{v}_{mk,s}\langle \chi_t|\mathrm{H}_{t,s\ \text{core}}|\chi_s\rangle \\ &= \textstyle\sum_{t,s}\mathrm{v}_{nj,t}\mathrm{v}_{mk,s}\beta_{t,s} \end{aligned} \quad (16)$$

The interaction matrix elements in $\mathbf{A}^{\mathrm{D}}$ differ from those of the ordinary monomer CI expression (eq 5), due to the presence of the σ terms. *These terms are zero when the SCF treatment includes the complete Hamiltonian.*[39,49] Here, however, we have started with a representation (eq 1) that diagonalizes the SCF Hamiltonian constructed from two non-interacting monomers.

We now diagonalize the portions of $\mathbf{A}^{\mathrm{D}}$ that are made up of $\mathbf{A}^{\mathrm{aa,aa}}$ and $\mathbf{A}^{\mathrm{bb,bb}}$. That is, we use the intermediate transformations

$$\Psi^a{}_i = \textstyle\sum_N \mathbf{c}_{i,N}{}^1\psi^{aa}{}_N \text{ and } \Psi^b{}_k = \sum_M \mathbf{c}_{k,M}{}^1\psi^{bb}{}_M \quad (17)$$

where $\mathbf{c}_{i,N}$ and $\mathbf{c}_{k,M}$ are the CI coefficient matrices for the individual monomers. This transformation can be written in matrix notation as $\mathbf{U} = \mathbf{L}^{-1}\mathbf{A}^{\mathrm{D}}\mathbf{L}$ where

$$\mathbf{L} = \begin{bmatrix} \mathbf{c}^a & 0 & 0 & 0 \\ 0 & \mathbf{c}^b & 0 & 0 \\ 0 & 0 & 1 & 0 \\ 0 & 0 & 0 & 1 \end{bmatrix} \quad (18)$$

and **1** is the unit matrix.

The new representation transforms $\mathbf{A}^{\mathrm{D}}$ to a matrix **U**

$$\mathbf{U} = \begin{array}{c} \begin{matrix} {}^1\Psi^a{}_i \cdots & {}^1\Psi^b{}_j \cdots & {}^1\psi^{ab}{}_{N'} \cdots & {}^1\psi^{ba}{}_{M'} \cdots \end{matrix} \\ \left[\begin{matrix} \Delta\mathbf{E}^a & \mathbf{U}^{\mathrm{ex}} & \multicolumn{2}{c}{\multirow{2}{*}{$\mathbf{U}^{\mathrm{loc,ct}}$}} \\ \mathbf{U}^{\mathrm{ex}} & \Delta\mathbf{E}^b & & \\ \multicolumn{2}{c}{\multirow{2}{*}{$\mathbf{U}^{\mathrm{ct,loc}}$}} & \mathbf{U}^{ab,ab} & \mathbf{U}^{ab,ba} \\ & & \mathbf{U}^{ba,ab} & \mathbf{U}^{ba,ba} \end{matrix}\right] \end{array} \quad (19)$$

where the excitation energies of the isolated monomers, $\Delta\mathbf{E}^a$ and $\Delta\mathbf{E}^b$, now appear as diagonal terms. Exciton interactions between the two molecules are described by $\mathbf{U}^{\mathrm{ex}}$, and $\mathbf{U}^{\mathrm{loc,ct}}$ represents the interactions between the diagonalized local transitions (Q_y, Q_x, B_x, and B_y) and the CT transitions. $\mathbf{U}^{ab,ab}$, $\mathbf{U}^{ba,ba}$, $\mathbf{U}^{ab,ba}$ and $\mathbf{U}^{ba,ab}$ are identical with the corresponding submatrices of $\mathbf{A}^{\mathrm{D}}$. Diagonalization of just the portion of **U** that is made up of $\Delta\mathbf{E}^a$, $\Delta\mathbf{E}^b$, and $\mathbf{U}^{\mathrm{ex}}$ is the solution of the familiar exciton problem. The evaluation of the matrix elements of **U** will be considered in the following section.

It is important to note that our selection of the molecular orbital coefficients ($\mathrm{v}_{n,t}$) and CI coefficients ($\mathrm{c}_{i,N}$) is based on the wave functions of the isolated monomers and not on the wave functions of the supermolecular oligomer. This selection provides a convenient zero-order basis set, allowing the interactions between the monomers, and the effects of these interactions on the wave functions, to be expressed in the interaction matrix **U**.

Interaction Matrix Elements. The diagonal matrix elements $\Delta\mathbf{E}^a$ and $\Delta\mathbf{E}^b$ are the excitation energies of the individual molecules. These energies are expected to depend somewhat on the polarizability of the neighboring molecules, as well as on the environment provided by the protein. Such environmental effects can be included at the level of the SCF treatment of the monomers if one has the X-ray coordinates of the protein.[50] Since the reaction center coordinates are still under refinement,[4,5] one can allow for environmental effects in an approximate way by introducing small shifts in the local excitation energies $\Delta\mathbf{E}^a$ and $\Delta\mathbf{E}^b$. For calculations on the reaction center,[34] the energies were chosen to match the corresponding absorption maxima of the monomeric pigments in solution, with minor adjustments to improve the agreement between the calculated and observed absorption bands. These adjustments will be discussed in the following paper.[34]

The off-diagonal elements of **U** can be evaluated by using eq 15 and 16 and summing over the terms of eq 12 and 17. Consider first the exciton-interaction submatrix $\mathbf{U}^{\mathrm{ex}}$, which describes the mixing of local state $\Psi^a{}_i$ of molecule a with state $\Psi^b{}_k$ of molecule b. Writing these states as in eq 17, and expanding the monomer wave functions as in eq 12, one obtains

$$\mathbf{U}^{\mathrm{ex}}{}_{i,k} = \langle \Psi^a{}_i|\mathrm{H}|\Psi^b{}_k\rangle = 2\textstyle\sum_{N,M}\mathrm{c}_{i,N}\mathrm{c}_{k,M}\sum_{s,t}\mathrm{v}_{m1,s}\mathrm{v}_{m2,s}\mathrm{v}_{n1,t}\mathrm{v}_{n2,t}\gamma_{s,t} \quad (20)$$

This standard transition-monopole expression comes from the term $2\langle \mathrm{m_1n_2}|\mathrm{m_2n_1}\rangle$ in eq 15, all the other terms evaluating to zero.

For the electron–electron repulsion integral, $\gamma_{s,t}$, we used the semiempirical expression

$$\gamma_{s,t} = [3.77 \times 10^4 \exp(-0.232 r_{s,t}/\text{Å}) + 1.17 \times 10^5/(2.82 + r_{\mathrm{s,t}}/\text{Å})]\ \mathrm{cm}^{-1} \quad (21)$$

where $r_{s,t}$ is the distance between atoms s and t.[30] Equation 21 reduces to e^2/r at large distances, and using this simpler expression for γ in eq 20 gives very similar results.

When monomers a and b are sufficiently far apart, the exciton interaction matrix elements should become equivalent to the in-

(49) Itoh, H.; I'Haya, Y. *Theor. Chim. Acta* **1964**, *2*, 247–257.

(50) Warshel, A.; Russell, S. T. *Q. Rev. Biophys.* **1984**, *17*, 283–422.

teraction energies ($U^{ex}_{i,k}$) calculated by using the transition dipoles in a point-dipole approximation

$$U^{ex}_{i,k} = (\mu^a_i \cdot \mu^b_k)/|r_{a,b}|^3 - 3(\mu^a_i \cdot r_{a,b})(\mu^b_k \cdot r_{a,b})/|r_{a,b}|^5 \quad (22)$$

where $r_{a,b}$ is the vector connecting the molecular centers. However, the transition-monopole and point-dipole treatments will converge in this way only if the calculated transition dipoles of the monomers are equal to the observed values. As noted above, calculations using the electron position opeator (eq 7) tend to overestimate the dipole strengths of the individual transitions. Since we are not trying to obtain the best results for the monomers ab initio, but rather to calculate the properties of the oligomer in a consistent way, we have followed Murrell and Tanaka[40] and have scaled eq 20 by a consistency factor Ω so that

$$U^{ex}_{i,k} = (\Omega^{a,b}_{i,k})(2\sum_{N,M} c_{i,N} c_{k,M} \sum_{s,t} v_{m1,s} v_{m2,s} v_{n1,t} v_{n2,t} \gamma_{s,t}) \quad (23a)$$

with

$$\Omega^{a,b}_{i,k} = [(D^a_{i,obsd}/D^a_{i,calcd})(D^b_{k,obsd}/D^b_{k,calcd})]^{1/2} \quad (23b)$$

Here $D^a_{i,obsd}$ and $D^b_{k,obsd}$ are the experimentally measured dipole strengths for transitions i and k, and $D^a_{i,calcd}$ and $D^b_{k,calcd}$ are the dipole strengths calculated with eq 7. This correction has been found to work well in descriptions of the excimer fluorescence of polycyclic aromatic molecules.[51] The correction factor Ω is typically about 0.5.

As was discussed above, the monomer transition dipoles calculated by the gradient operator (eq 8) rather than the position operator (eq 7) do agree well with the experimental values. The CI coefficients have been adjusted to maximize this agreement. However, the exciton interaction matrix elements are more directly related to the position operator and should therefore be scaled accordingly. The fact that the gradient operator allows a reliable estimate of the transition dipole can be exploited to obtain Ω for the B_x and B_y transitions; for these transitions we used the dipole strengths calculated with the gradient operator in place of $D^a_{i,obsd}$ and $D^b_{k,obsd}$, since the experimental values are uncertain.

Figure 2 shows that the transition-monopole treatment converges with the point-dipole treatment when molecules *a* and *b* are sufficiently far apart. Curve 1 in Figure 2A shows the corrected transition-monopole matrix elements for the interaction of the Q_y transitions of two molecules of BChl-*b* as a function of the intermolecular distance. The point-dipole interaction energies are plotted as curve 2. Figure 2B shows a similar comparison for the Q_x transitions. The geometry of the dimer used for these calculations is based on that of the special pair of BChl-*b* molecules ($BChl_{LP}$ and $BChl_{MP}$) in the *Rps. viridis* reaction center[4,5] (Figure 1B). To generate Figure 2, $BChl_{MP}$ was moved along the axis given by the cross product of the N1 → N3 vectors of the two molecules. The transition-monopole and point-dipole energies converge when the molecules are far apart, as they should, but they can differ significantly at the short distance that applies in the reaction center (3.1 Å). One would not expect the point-dipole approximation to be reliable when the molecules are this close together, because the molecular dimensions are on the order of 10 Å (Figure 1).

We now turn to the $U^{ab,ab}$ and $U^{ba,ba}$ submatrices, which describe intermolecular CT transitions. A BChl dimer has four principal singlet CT transitions, $^1\psi^{ab}_N$, in which an electron is excited from SCF orbital ϕ^a_{n1} of BChl *a* to orbital ϕ^b_{n2} of BChl *b*. The lowest energy CT state involves excitation of an electron from ϕ^a_2 to ϕ^b_3 (Figure 3). The second involves excitation from ϕ^a_1 to ϕ^b_3; and the third and fourth involve excitation from ϕ^a_2 and ϕ^a_1 to ϕ^b_4. There also are four corresponding transitions, $^1\psi^{ba}_M$, in which an electron moves from SCF orbital ϕ^b_{m1} of BChl *b* to orbital ϕ^a_{m2} of BChl *a*. The energies of the CT transitions constitute the diagonal elements of $U^{ab,ab}$ and $U^{ba,ba}$. For a dimer in a vacuum, these energies can be calculated with eq 5a. The term $2\langle n_1 n_2 | n_2 n_1 \rangle$ is zero for an intermolecular CT transition, and the term $\langle n_1 n_2 | n_1 n_2 \rangle$ becomes $\sum_{t,s}(v_{n1,t})^2(v_{n2,s})^2\gamma_{t,s}$. Thus we obtain

$$U^{ab,ab}_{N,N} = \langle \Psi^{ab}_N | H | \Psi^{ab}_N \rangle = E_{n2} - E_{n1} + \sum_{t,s}(v_{n1,t})^2(v_{n2,s})^2\gamma_{t,s} \quad (24)$$

The orbital energy differences ($E_{n2} - E_{n1}$) obtained in the original diagonalization of **F** (eq 2) were approximately 36 000 cm^{-1} (for transfer from ϕ^a_2 to ϕ^b_3), 41 000 cm^{-1} (ϕ^a_1 to ϕ^b_3), 51 000 cm^{-1} (ϕ^a_2 to ϕ^b_4), and 55 000 cm^{-1} (ϕ^a_1 to ϕ^b_4). However, these numbers probably are reliable only to within about ±4000 cm^{-1}. Judging from the tendency of the calculations to overestimate the Q_y excitation energy, the calculated energy difference between ϕ_2 and ϕ_3 appears to be too large by about 3000 cm^{-1}, whereas that between ϕ_1 and ϕ_3 appears to be more accurate. We therefore chose trial values of 33 000 cm^{-1} for $E_{\phi 3} - E_{\phi 2}$, 41 000 cm^{-1} for $E_{\phi 3} - E_{\phi 1}$, 46 000 cm^{-1} for $E_{\phi 4} - E_{\phi 2}$, and 54 000 cm^{-1} for $E_{\phi 4} - E_{\phi 1}$. With the geometry shown in Figure 1B (3.1 Å between the planes of the two BChl molecules), the calculated CT energies ($U^{ab,ab}_{N,N}$) then are found to be 13 400 cm^{-1} (for transfer from ϕ^a_2 to ϕ^b_3), 21 300 cm^{-1} (ϕ^a_1 to ϕ^b_3), 27 600 cm^{-1} ϕ^a_2 to ϕ^b_4), and 35 800 cm^{-1} (ϕ^a_1 to ϕ^b_4). Curve 1 in Figure 3A shows how the calculated energy of the lowest CT transition depends on the intermolecular distance. The two molecules are moved apart along the same axis as was used for Figure 2. For reference, curves 2–5 in Figure 3A show the energies of the four lowest exciton states if the CT transitions are not allowed to interact with the local transitions. As noted above, these energies are obtained by di-

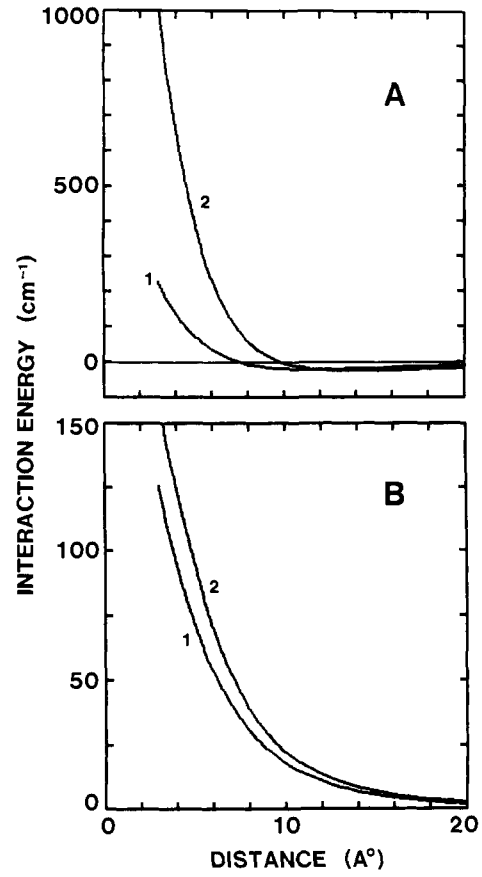

Figure 2. (A) Distance dependence of the matrix elements describing the interaction of the Q_y transitions of $BChl_{LP}$ and $BChl_{MP}$ of the *Rps. viridis* reaction center, as calculated by a transition-monopole treatment (eq 23, curve 1) and by a point-dipole treatment (eq 22 with the transition dipoles obtained with eq 8, curve 2). The geometry of the complex is illustrated in Figure 1B. $BChl_{MP}$ is translated along the axis shown with a dashed line in that figure. The abscissa is the length of the vector connecting the molecular centers, as projected on the translation axis. In the X-ray structure, the center-to-center distance is 7.1 Å, and the projection on the translation axis is approximately 3.1 Å. (B) Matrix elements for interaction of the Q_x transitions of $BChl_{LP}$ and $BChl_{MP}$. Other conditions as in part A.

(51) Azumi, T.; Armstrong, A. T.; McGlynn, S. P. *J. Chem. Phys.* **1964**, *41*, 3839–3852.

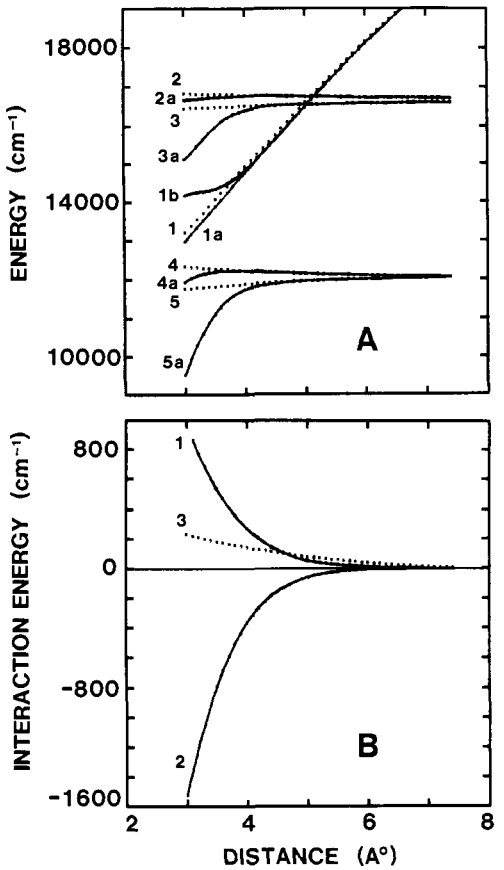

Figure 3. (A) Curve 1: Energy of the CT basis transition in which an electron moves from ϕ_2 of $BChl_{LP}$ to ϕ_3 of $BChl_{MP}$, or vice versa, as calculated with eq 5A. The differences between the molecular orbital energies ($E_{n2} - E_{n1}$) are fixed as described in the text. To show the distance dependence of the energy, $BChl_{MP}$ is translated along the same axis as used for Figure 2. This calculation does not consider the interactions of the different CT transitions, or the solvation of the charged species by the protein. Curves 2, 3, 4, and 5: Distance dependence of the calculated energies of the four lowest exciton states of the same dimer, when CT transitions are omitted from the calculation. The interaction matrix elements were obtained by the transition-monopole treatment, as for curve 1 in parts A and B of Figure 2. Curves 2a, 3a, 4a, and 5a: Calculated energies of the four corresponding states of the dimer when CT transitions are included. Curves 1a and 1b: Energies of the dimer's pair of transitions corresponding to curve 1 when the CT transitions are allowed to interact with each other and with the local transitions. These two transitions split apart in energy at short intermolecular distances, when interactions with the local transitions become appreciable. For a dimer with C_2 symmetry, one component contains a symmetric combination of the basis CT transitions in opposite directions between the two BChls, and the other contains an antisymmetric combination. If the dimer is asymmetric, the two curves generally will be separated in energy even at large intermolecular distances. (B) Curve 1: Matrix element for the interaction of the Q_y transition of $BChl_{LP}$ with the CT transition in which an electron moves from ϕ_2 of this BChl to ϕ_3 of $BChl_{MP}$, as calculated with eq 27. $BChl_{MP}$ is translated as in Figure 2. Curve 2: Matrix element for the interaction of the Q_y transition of $BChl_{LP}$ with the CT transition in which an electron moves from ϕ_2 of $BChl_{MP}$ to ϕ_3 of $BChl_{LP}$, as calculated with eq 28. Other conditions as for curve 1. Curve 3: corrected point-monopole matrix element for the interaction of the Q_y transitions of $BChl_{LP}$ and $BChl_{MP}$, replotted from Figure 2A.

agonalizing the submatrix made up of $\Delta\mathbf{E}^a$, $\Delta\mathbf{E}^b$, and $\mathbf{U}^{ex}$. The exciton states represented by curves 2 and 3 are made up largely of the local Q_x transitions of the two molecules, with small contributions from the Q_y, B_x, and B_y transitions. Those represented by curves 4 and 5 consist primarily of the Q_y transitions, with smaller contributions from Q_x, B_x, and B_y. The additional curves in Figure 3A will be discussed below.

The energies of the CT transitions in the reaction center are expected to be much less sensitive to the intermolecular distance than curve 1 of Figure 3A, because the two radicals can be stabilized by interactions with polar and polarizable groups of the protein. The solvation energies cannot yet be calculated accurately, in part because we have insufficient information on the structure of the protein. In the following paper,[34] we therefore vary the energies of the CT transitions and consider how this affects the calculated absorption and CD spectra.

The off-diagonal elements of $\mathbf{U}^{ab,ab}$ and $\mathbf{U}^{ba,ba}$ describe the mixing of different CT transitions in the same direction. These can be evaluated by using eq 16. The result is

$$\mathbf{U}^{ab,ab}{}_{W,N} = \langle {}^1\psi^{ab}{}_W|\mathrm{H}|{}^1\psi^{ab}{}_N\rangle = -\sum_{t,s} v_{n1,t} v_{w1,t} v_{n2,s} v_{w2,s} \gamma_{t,s} \quad (25)$$

where ${}^1\psi^{ab}{}_W$ represents a different excitation in the same direction as ${}^1\psi^{ab}{}_N$ (from $\phi^a{}_{w1}$ to $\phi^b{}_{w2}$). This expression comes from the final term in eq 15; all the other terms are zero.

The matrix elements of $\mathbf{U}^{ab,ba}$, which describe the mixing of CT transitions in opposite directions, are evaluated similarly, with the result

$$\mathbf{U}^{ba,ab}{}_{M,N} = ({}^1\psi^{ba}{}_M|\mathrm{H}|{}^1\psi^{ab}{}_N\rangle = 0 \quad (26)$$

Now consider the $\mathbf{U}^{loc,ct}$ submatrix, which describes the interactions of $\Psi^a{}_i$ and $\Psi^b{}_k$ with the CT transitions. Expanding $\Psi^a{}_i$, $\phi^a{}_{w1}$, and $\phi^b{}_{w2}$ in terms of $\chi^a{}_t$ and $\chi^b{}_s$ as in eq 17 and 12, and inserting the orbitals into eq 15 and 16, one obtains

$$\begin{aligned} \mathbf{U}^{a,ab}{}_{i,W} &= \langle \Psi^a{}_i|\mathrm{H}|{}^1\psi^{ab}{}_W\rangle = \sum_N c_{i,N}\delta_{n1,w1}\sigma_{n2,w2} \\ &= \sum_N c_{i,N}\delta_{n1,w1}\sum_{s,t} v_{n2,t} v_{w2,s}\beta_{s,t} \end{aligned} \quad (27)$$

All the other terms evaluate to zero. Similarly, for electron transfer in the opposite direction

$$\begin{aligned} \mathbf{U}^{a,ba}{}_{i,M} &= (\Psi^a{}_i|\mathrm{H}|{}^1\psi^{ba}{}_M\rangle = -\sum_N c_{i,N}\delta_{n2,m2}\sigma_{n1,m1} \\ &= -\sum_N c_{i,N}\delta_{n2,m2}\sum_{s,t} v_{n1,t} v_{m1,s}\beta_{s,t} \end{aligned} \quad (28)$$

Figures 4 and 5 illustrate the application of eq 27 and 28 for the case of the interaction between the Q_y transition of $BChl_{LP}$ and the CT transitions in which an electron is transferred from ϕ_2 of this BChl to ϕ_3 of $BChl_{MP}$ (Figures 4A and 5A) or, in the opposite direction, from ϕ_2 of $BChl_{MP}$ to ϕ_3 of $BChl_{LP}$ (Figures 4B and 5B). With the simplified set of CI coefficients that we used (Table II), the sum over N always reduces to a single term.

The resonance integral, $\beta_{s,t}$, can be evaluated by dividing it into σ and π components

$$\beta_{s,t} = \beta_\sigma \eta_{z',s}\eta_{z',t} + \beta_\pi(\eta_{x',s}\eta_{x',t} + \eta_{y',s}\eta_{y',t}) \quad (29)$$

where $\beta_\sigma = \int p_z H_{core} p_z \, d\tau$, $\beta_\pi = \int p_x H_{core} p_x \, d\tau$, and $(\eta_{x',s}, \eta_{y',s}, \eta_{z',s})$ and $(\eta_{x',t}, \eta_{y',t}, \eta_{z',t})$ are the direction cosines of the p_z orbitals on atoms s and t, with respect to a rectangular coordinate system (x', y', z') defined so that the z' axis is along the line between atoms s and t. The semiempirical integrals β_σ and β_π are

$$\begin{aligned} \beta_\sigma = \exp(-\rho_\sigma/2)[&8.512 \times 10^4 + 4.255 \times 10^4\rho_\sigma + 4.255 \times \\ &10^3\rho_\sigma{}^2 - 1.418 \times 10^3\rho_\sigma{}^3 - 3.546\times 10^2\rho_\sigma{}^4] \text{ cm}^{-1} \end{aligned} \quad (30)$$

with $\rho_\sigma = 5.385\, r_{s,t}/\text{Å}$, and

$$\beta_\pi = 3.108 \times 10^5 \exp(-1.95 r_{s,t}/\text{Å}) \text{ cm}^{-1} \quad (31)$$

β_π is the standard resonance integral used in the QCFF/PI calculations for π interactions.[30,31] β_σ is the resonance integral for two end-on p_z orbitals ($\mathbf{z} = \mathbf{z}'$), which has been parametrized previously by fitting calculated and observed properties of pyrene and other excimers.[47,48]

Curve 1 in Figure 3B shows the distance dependence of the matrix element that mixes the Q_y transition of $BChl_{LP}$ with the CT transition in which an electron moves from ϕ_2 of $BChl_{LP}$ to ϕ_3 of $BChl_{MP}$. (This is the same matrix element that is illustrated in Figures 4A and 5A.) Curve 2 shows the matrix element for mixing the same CT transition with the Q_y transition of $BChl_{MP}$; this is identical with the element illustrated in Figures 4B and 5B. To explore the distance dependence, the two molecules are moved apart along the same axis that is used in Figures 2 and 3A. At the short distance that is found between $BChl_{LP}$ and $BChl_{MP}$ in the reaction center, the matrix elements between CT

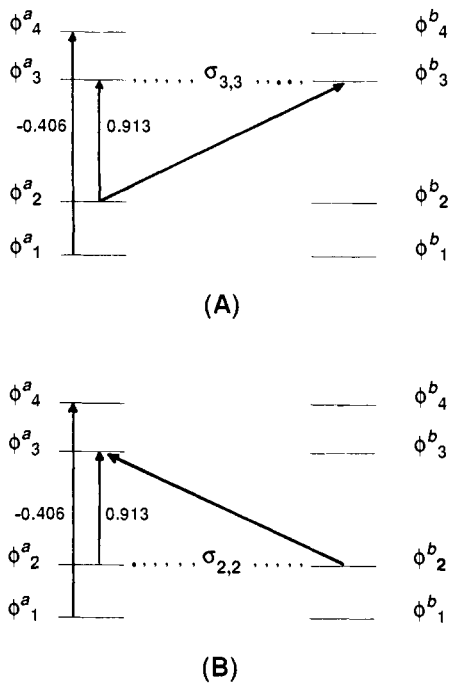

Figure 4. (A) In the four-orbital model, the lowest energy CT transition of a BChl dimer involves excitation of an electron from ϕ^a_2 to ϕ^b_3 (diagonal arrow). The Q_y transition of molecule *a* consists mainly of excitations (vertical arrows) from ϕ^a_2 to ϕ^a_3 (CI coefficient $c_{l,N}$ = 0.913, Table II) and from ϕ^a_1 to ϕ^a_4 (CI coefficient = -0.408). The matrix elements describing the interactions of a local transition of BChl *a* with the CT transition ψ^{ab}_W depend on the terms $\delta_{n1,w1}\sigma_{n2,w2}$ (eq 27). For the pair of transitions illustrated here, the delta function $\delta_{n1,w1}$ is 1 for the component of the Q_y transition involving excitation from ϕ^a_2 to ϕ^a_3 (the initial orbitals are the same in the CT and local transitions) and zero for the component involving excitation from ϕ^a_1 to ϕ^a_4. The interaction matrix element thus depends on the overlap between the two final orbitals, ϕ^a_3 and ϕ^b_3 ($\sigma_{3,3}$, dotted line). (B) The same Q_y transition also interacts with the CT transition (ψ^{ba}_M) in which an electron is transferred from ϕ^b_2 to ϕ^a_3. The delta function $\delta_{n2,m2}$ in eq 28 is 1 for the component of the Q_y transition involving excitation from ϕ^a_2 to ϕ^a_3. The interaction matrix element thus depends on the overlap between the two initial orbitals ϕ^a_2 and ϕ^b_2 ($-\sigma_{2,2}$). The component of the Q_y transition involving excitation from ϕ^a_1 to ϕ^a_4 mixes the Q_y transition with higher energy CT states in which an electron is excited from ϕ^a_1 or to ϕ^a_4.

and local transitions can be significantly greater than the exciton interaction matrix elements (e.g., curve 3 in Figure 3B), but they fall off more rapidly with distance.

It is reasonable to ask whether the elements of $\mathbf{U}^{loc,ct}$ require correction factors analogous to Ω. The answer in principle is no, because the overlap integrals β_σ and β_π have already been parametrized to adjust the sizes of these elements.[47,48] However, the data set used for the parametrization is limited, and the reliability of the parameters can be determined only by testing them in new cases such as the present one. It does seem likely that the off-diagonal elements of $\mathbf{U}^{ab,ab}$ and $\mathbf{U}^{ba,ba}$ (eq 25) require some correction, but there is no simple way to relate these terms uniquely to experimentally observable parameters. In the calculations on reaction centers to be described in the following paper,[34] decreasing the off-diagonal elements of $\mathbf{U}^{ab,ab}$ and $\mathbf{U}^{ba,ba}$ by a factor of 2 had relatively little effect on the results.

Excited States and Ground State of the Oligomer. The excited states of a dimer or higher oligomer now can be described as

$$\vartheta_i = \sum_j C_{i,j}\xi_j \tag{32}$$

where the ξ_j are the local and CT transitions that form the basis of **U**. The coefficients $C_{i,j}$ and the excitation energies ΔE^T_i are the solutions of

$$\mathbf{UC}_i = \Delta E^T_i \mathbf{C}_i \tag{33}$$

and are obtained by diagonalizing **U**. Although **U** has been written here for a dimer, it can be expanded straightforwardly to larger

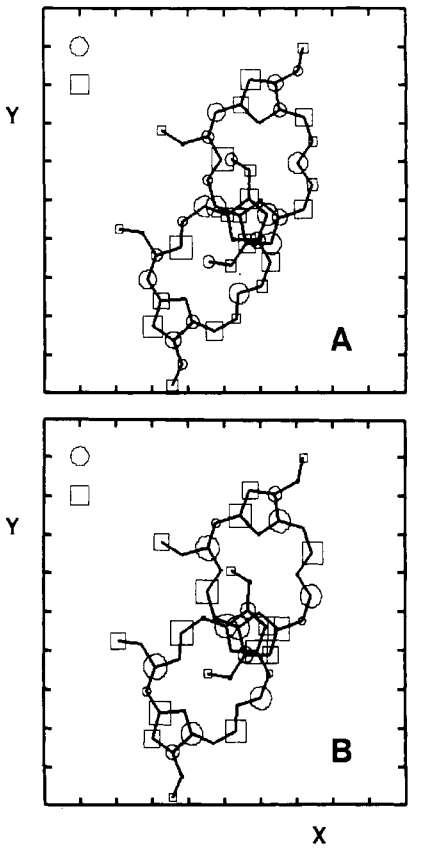

Figure 5. The overlap term $\sigma_{n2,w2}$ in eq 27 depends on the molecular orbital expansion coefficients, $v_{n2,t}$ and $v_{w2,s}$, and on the p_z resonance integrals, $\beta_{s,t}$. The molecular orbital coefficients (Table I) are illustrated here for the special pair of BChls in the *Rps. viridis* reaction center. In drawing A, the circle or square at each atomic position has a diameter or edge proportional to the amplitude of the coefficient for orbital ϕ_3 at that atom. Circles represent coefficients with positive signs and squares coefficients with negative signs. The circle and square at the upper left indicate the scales for coefficients of ±0.5. The largest contributions to the interaction matrix element considered in Figure 4A come from regions where the symbols associated with the two molecules overlap. The coordinate system for the drawing is the same as that in Figure 1; $BChl_{LP}$ is the upper molecule in the figure. Drawing B shows the amplitudes of the molecular orbital coefficients for ϕ_2, which enter in eq 28 and Figure 4B.

oligomers. For a BChl dimer, the set of ξ_j consists of 8 local transitions and 8 CT transitions. For the complex of four BChl and two BPh molecules in the reaction center, ξ_j includes 24 local transitions and 120 CT transitions. However, because of the steep distance dependence of the resonance integrals (Figure 3B), the only CT states that have a significant influence on the absorption spectrum are those involving electron transfer between $BChl_{LP}$ and $BChl_{MP}$. We have therefore included only these 8 of the CT states in most of the calculations described in the following paper.[34] This reduces **U** to a 32 × 32 matrix.

Curves 1a, 1b, 2a, 3a, 4a, and 5a in Figure 3A show the excitation energies ΔE^T_i for the first 6 excited states of the BChl dimer that is illustrated in Figure 1B. At intermolecular distances much greater than about 5 Å, the energies of the first 4 transitions (curves 2a–5a) are essentially the same as the energies of the exciton transitions that are obtained by omitting CT transitions from **U** (curves 2–5); the fifth and sixth transitions are almost purely CT in character and are nearly degenerate (curves 1a and 1b). (For these calculations, the CT basis transitions in which an electron moves from molecule *a* to molecule *b* were assumed to have the same energies as the corresponding transitions in which an electron moves in the opposite direction. This point will be discussed in more detail in the following paper.[34]) Curves 1a and 1b lie slightly below curve 1, which gives the energy of the lowest CT basis transition, as a result of configuration interaction with the higher CT transitions. As the two molecules are moved closer

together, the exciton transitions and CT transitions begin to interact, and the excited states begin to be strongly mixed in character. Curves 1a and 1b split apart in energy, and curves 2a–5a bend downward.

In order to calculate the spectroscopic properties of the oligomer, one also must consider how intermolecular interactions affect the ground state of the complex. The zero-order wave function for the ground state of the complex is simply

$$\vartheta_0 = \Pi_a \Psi^a{}_0 \tag{34}$$

where $\Psi^a{}_0$ is the zero-order ground state of molecule a. However, ϑ_0 interacts with doubly excited states, $\Psi^a{}_j\Psi^b{}_k\Pi_{c\neq a\neq b}\Psi^c{}_0$, in which molecules a and b are raised to states $\Psi^a{}_j$ and $\Psi^b{}_k$. For a complex of 6 porphyrins such as the reaction center, there are 240 such doubly excited states. Because these states lie well above ϑ_0 in energy, their individual contributions to the ground state are small and can be found by first-order perturbation theory.[19,52] The coefficient for the contribution of $\Psi^a{}_j\Psi^b{}_k\Pi_{c\neq a\neq b}\Psi^c{}_0$ is given approximately by

$$G^{a,b}{}_{j,k} = -[\langle \Psi^a{}_j|\mathrm{U}|\Psi^b{}_k\rangle/(\Delta E^a{}_j + \Delta E^b{}_k)]G_0 \tag{35}$$

where

$$G_0 = \{1 + \sum_{a,b,j,k}[\langle \Psi^a{}_j|\mathrm{U}|\Psi^b{}_k\rangle/(\Delta \mathrm{E}^a{}_j + \Delta E^b{}_k)]^2\}^{-1/2} \tag{36}$$

The terms $\langle \Psi^a{}_i|\mathrm{U}|\Psi^b{}_k\rangle$ in eq 35 and 36 are the matrix elements of U^{ex} (eq 23a). G_0 is a renormalization factor that expresses the relative contribution of the zero-order state (ϑ_0) to the first-order ground state. For the reaction center, G_0 is found to be about 0.997, which is, as expected, very close to 1. Even so, doubly excited states can contribute significantly to the calculated CD spectrum.[19]

Spectroscopic Properties of the Oligomer. The electric and magnetic transition dipoles for excitation of the complex to state ϑ_i are obtained by summing the transition dipoles of the individual molecules ($\mu^a{}_j$ and $\mathbf{m}^a{}_j$, as obtained with eq 8 and 10), weighting the contribution of each local transition (ξ_j) by $\mathrm{C}_{i,j}$ (as obtained with eq 32 and 33), and including the contributions from downward transitions of the doubly excited states that are part of the ground state (eq 35)

$$\mu^{\mathrm{T}}{}_i = \sum_{a,j}\{G_0\mathrm{C}^a{}_{i,j} + \sum_{b\neq a}\sum_k G^{a,b}{}_{j,k}\mathrm{C}^b{}_{i,k}\}\mu^a{}_j \tag{37}$$

and

$$\mathbf{m}^{\mathrm{T}}{}_i = \sum_{a,j}\{G_0\mathrm{C}^a{}_{i,j} - \sum_{b\neq a}\sum_k G^{a,b}{}_{j,k}\mathrm{C}^b{}_{i,k}\}\mathbf{m}^a{}_j \tag{38}$$

where the $\mathrm{C}^a{}_{i,j}$ are the coefficients associated with the four local transitions of molecule a, and $\mathrm{C}^b{}_{i,k}$ are those associated with those of molecule b. Contributions from downward transitions enter the magnetic transition dipole (eq 38) with negative signs because of the imaginary nature of the momentum operator (eq 10). The importance of including the B_x and B_y transitions even if one is interested mainly in the spectra at long wavelengths has been discussed previously.[19] The CT transitions have very small intrinsic transition dipoles and do not need to be included explicitly in eq 37 and 38, but they do participate in eq 32 and 33, and they can have strong effects on the excitation energies ($\Delta E^{\mathrm{T}}{}_i$) and coefficients ($\mathrm{C}_{i,j}$) for the excited states. Absorption bands that are largely CT in character gain dipole strength to the extent that they contain contributions from the local π–π^* states.

Linear dichroism can be calculated from the components of $\mu^{\mathrm{T}}{}_i$ parallel and perpendicular to any particular vector of interest, such as the C_2 symmetry axis of the reaction center. Rotational strengths, $\mathcal{R}^{\mathrm{T}}{}_i$, are obtained from the scalar product of $\mu^{\mathrm{T}}{}_i$ and $\mathbf{m}^{\mathrm{T}}{}_i$, just as in eq 11. By using eq 10 to obtain the magnetic transition dipoles of the individual molecules ($\mathbf{m}^a{}_j$), we have included the intrinsic rotational strengths of the monomers in $\mathcal{R}^{\mathrm{T}}{}_i$, along with the rotational strength that arises from exciton interactions.

The change in permanent dipole moment associated with an absorption band of the oligomer, $\Delta\mu^{\mathrm{T}}{}_i$, is given approximately by

$$\Delta\mu^{\mathrm{T}}{}_i \approx G_0\sum_{j,k}\mathrm{C}_{i,j}\mathrm{C}_{i,k}\Delta\mu_{j,k} \tag{39}$$

where

$$\Delta\mu_{j,k} = e\sum_{N,M,t}\mathrm{c}_{j,N}\mathrm{c}_{k,M}(\delta_{n1,m1}\mathrm{v}_{n2,t}\mathrm{v}_{m2,t} - \delta_{n2,m2}\mathrm{v}_{n1,t}\mathrm{v}_{m1,t})\mathrm{r}_t \tag{40}$$

The diagonal terms ($\Delta\mu_{j,j}$) are the changes in permanent dipole moment in the basis transitions. Contributions of the doubly excited states to $\Delta\mu^{\mathrm{T}}{}_i$ are small, and they have been neglected in eq 39. The changes in permanent dipole moment associated with the CT transitions of the reaction center are considerably larger than the changes associated with the local transitions. For the transfer of an electron from ϕ_2 of $\mathrm{BChl}_{\mathrm{MP}}$ to ϕ_3 of $\mathrm{BChl}_{\mathrm{LP}}$, $|\Delta\mu|$ is calculated to be 32.3 D, compared to about 0.7 and 2.3 D for the Q_y and Q_x transitions of the individual BChl-*b* molecules. The admixture of CT transitions thus is expected to make some of the reaction center's absorption bands especially sensitive to external electric fields.

Concluding Remarks

Until recently, it was not possible to predict the detailed properties of large molecules with reasonable accuracy. One could, of course, adopt the approach of fitting the properties of such a molecule to a phenomenological model with adjustable parameters, using the fitting to extract the best values of the parameters. In the case of a bacteriochlorophyll dimer, this is equivalent to taking the observed red shift and rotational strength of the long-wavelength absorption band and extracting an effective transition dipole moment or the intermolecular distance and orientation.[2,9–11,14–16,18–20] Though instructive, the phenomenological approach can offer only limited insight into the detailed interactions in a complicated biological system, and it does not provide a reliable way of predicting the detailed properties of new systems. For example, if the model does not include charge-transfer interactions, it may still give a good fit to the observed spectra by using overestimates of the transition dipoles, but it will not account satisfactorily for the dipole moments of the excited states and it will not enable one to calculate rates of electron transfer.

At the opposite extreme, the philosophy of the ab initio approach is to solve the quantum mechanical problem exactly. Unfortunately, large molecular systems are not presently tractable in this way, because accurate calculations require very large basis sets and a vast number of configurations. If the basis set is made small enough to be manageable, the calculated excitation energies for a porphyrin monomer are typically in error by 40%.[28] If one applies empirical corrections for this error, the "ab initio" calculations become, in the end, no more rigorous or informative than the semiempirical treatment that we have used in the present work. More importantly, moving from monomers to larger systems is not possible by the ab initio approach. The most that one could do would be to take the ab initio wave functions of the monomers and use them to analyze the intermolecular interactions by procedures similar to those described here.

The problems associated with the phenomenological and ab initio approaches have led to the development of the intermediate semiempirical approach (for a review, see ref 32). The philosophy here is that a complicated system can be studied on a very detailed level, provided that detailed information about the components of the system is transferred from studies of the isolated components.[32] Instead of calculating the properties of bacteriochlorophyll monomers from first principles, one can fit the best set of semiempirical integrals to the properties of the monomers and related molecules. The key principle of the semiempirical approach is *not* to fit the parameters to the problem under study. For example, the parameters in the semiempirical integrals are not adjustable parameters in studies of the oligomers. To study the reaction center by the semiempirical approach, we have attempted to obtain as unbiased and consistent a model as possible. The only adjustable parameters at the level of the oligomer are the diagonal matrix elements of U, which are expected to depend strongly on the solvation of the monomers by the protein microenvironment.

(52) Tinoco, I. *Adv. Chem. Phys.* **1962**, *4*, 113–157.

Calculations of these solvation energies should be possible when the protein structure becomes available.[50]

As shown in Figure 3A, charge-transfer transitions within the special pair of BChls ($BChl_{LP}$ and $BChl_{MP}$) are expected to have significant effects on the reaction center's spectroscopic properties. We shall analyze these effects further in the following paper[34] and shall show that the theory developed here accounts well for the main features of the absorption, linear dichroism, and circular dichroism spectra of the *Rps. viridis* reaction center. This detailed comparison of the model with experiment is necessary, in order to assess the reliability of the interaction matrix elements. This is critical to an understanding of the initial steps of photosynthesis, because the same type of matrix elements are involved in governing the rate of intermolecular electron transfer.[53,54]

Acknowledgment. This work was supported by National Science Foundation Grants PCM-8303385, PCM-8312371 and PCM-8316161. We also acknowledge with thanks the help of the ISIS program from Digital Equipment Corp. in obtaining the MicroVax II computer on which many of the calculations were done. We thank J. Deisenhofer and H. Michel for providing the crystallographic coordinates, S. Creighton for help with the QCFF/PI calculations, and M. Gouterman, D. Middendorf, R. Pearlstein, and A. Scherz for helpful discussion.

(53) Warshel, A.; Schlosser, D. W. *Proc. Natl. Acad. Sci. U.S.A.* **1981**, *78*, 5564-5568.
(54) Parson, W. W.; Creighton, S.; Warshel, A. In *Primary Processes in Photobiology* Kobayashi, T., Ed.; Springer-Verlag: New York, in press.

Spectroscopic Properties of Photosynthetic Reaction Centers. 2. Application of the Theory to *Rhodopseudomonas viridis*

William W. Parson*† and Arieh Warshel*‡

Contribution from the Department of Biochemistry, University of Washington, Seattle, Washington 98195, and the Department of Chemistry, University of Southern California, Los Angeles, California 90007. *Received November 20, 1986*

Abstract: In the preceding paper [Warshel and Parson, companion paper], a nonphenomenological molecular theory is developed to calculate the spectroscopic properties of the reaction centers of photosynthetic bacteria. We here apply the theory to the reaction center of *Rhodopseudomonas viridis*, whose structure is known from recent X-ray crystallographic studies. Optical absorption, linear dichroism, and circular dichroism spectra are calculated and are compared with the spectra observed experimentally. Intermolecular charge-transfer (CT) transitions between the two bacteriochlorophylls (BChls) of the photochemically reactive special pair ($BChl_{LP}$ and $BChl_{MP}$) appear to make major contributions to the spectroscopic properties. Estimates of the energies of the CT transitions are obtained by exploring how these energies influence the calculated spectra. Good agreement with the observed spectra is obtained by placing the lowest energy CT transition from $BChl_{MP}$ to $BChl_{LP}$ near 14000 cm^{-1}, well above the reaction center's lowest excited state (10400 cm^{-1}), and placing the corresponding CT transition from $BChl_{LP}$ to $BChl_{MP}$ at a substantially higher energy. A large contribution of CT transitions to the reaction center's long-wavelength absorption band is consistent with recent hole-burning experiments and with the sensitivity of this band to external electric fields. Charge-transfer transitions involving the other two BChls ($BChl_{LA}$ and $BChl_{MA}$) are found not to contribute significantly to the spectra. To illustrate the sensitivity of the results to structural features, spectra are calculated as a function of the position of $BChl_{MP}$ and of the orientations of the acetyl groups of $BChl_{LP}$ and $BChl_{MP}$. To model the absorption changes that occur when the special pair of BChls is photooxidized, or when one of the two bacteriopheophytins is reduced, calculations are performed in which one or more of the molecules are omitted from the structure. The absorption changes that occur in the region from 790 to 860 nm reflect a strong mixing of the transitions of all six pigments.

The photosynthetic reaction center of *Rhodopseudomonas viridis* contains four molecules of bacteriochlorophyll *b* (BChl-*b*), two molecules of bacteriopheophytin *b* (BPh-*b*), two quinones, and one atom of non-heme iron, all bound to three polypeptides (L, M, and H). A fourth polypeptide houses four *c*-type hemes. The crystal structure of the reaction center has been solved by X-ray diffraction.[1-3] Two of the four BChls ($BChl_{LP}$ and $BChl_{MP}$) form a closely interacting "special pair" (P) that releases an electron when the reaction center is excited with light. The electron settles on one of the BPhs (BPh_L) with a time constant of about 3 ps[4-6] and then moves to one of the quinones in about 200 ps.[7] The other two BChls ($BChl_{LA}$ and $BChl_{MA}$) sit close by the reactive components,[1-3] but their roles in the electron-transfer reactions are still unclear.

The spectroscopic properties of bacterial reaction centers differ significantly from those of the isolated pigments and have remained poorly understood despite numerous experimental and theoretical studies (see references in the preceding paper[8]). The availability of a crystal structure has now made it possible to explore the spectroscopic properties of the *Rps. viridis* reaction center via detailed theoretical calculations. Such calculations are likely to be most informative if they aim to reproduce the experimental spectra by using calculated molecular parameters or unadjusted experimental parameters obtained with the isolated molecules in solution. This is a more challenging task then the conventional practice of fitting parameters to the observed spectra.

In the preceding paper[8] we developed a theoretical approach capable of predicting the spectra of oligomers of chlorophyll on

† University of Washington.
‡ University of Southern California.

(1) Deisenhofer, J.; Epp, O.; Miki, K.; Huber, R.; Michel, H. *J. Mol. Biol.* **1984**, *180*, 385-398.
(2) Deisenhofer, J.; Epp, O.; Miki, K.; Huber, R.; Michel, H. *Nature (London)* **1985**, *318*, 618-624.
(3) Michel, H.; Epp, O.; Deisenhofer, J. *EMBO J.* **1986**, *5*, 2445-2451.
(4) Woodbury, N. W.; Becker, M.; Middendorf, D.; Parson, W. W. *Biochemistry* **1985**, *24*, 7516-7521.
(5) Martin, J.-L.; Breton, J.; Hoff, A.; Migus, A.; Antonetti, A. *Proc. Natl. Acad. Sci. U.S.A.* **1986**, *83*, 957-961.
(6) Breton, J.; Martin, J.-L.; Migus, A.; Antonetti, A.; Orszag, A. *Proc. Natl. Acad. Sci. U.S.A.* **1986**, *83*, 5121-5125.
(7) Holten, D.; Windsor, M. W.; Parson, W. W.; Thornber, J. P. *Biochim. Biophys. Acta* **1978**, *501*, 112-126.
(8) Warshel, A.; Parson, W. W. *J. Am. Chem. Soc.*, preceding paper in this issue.

0002-7863/87/1509-6152$01.50/0